PLOS ONE

RESEARCH ARTICLE

Functional diversity of PFKFB3 splice variants in glioblastomas

Ulli Heydasch[1], Renate Kessler[1], Jan-Peter Warnke[2], Klaus Eschrich[1], Nicole Scholz[1‡*], Marina Bigl[1‡*]

1 Division of General Biochemistry, Rudolf Schönheimer Institute of Biochemistry, Faculty of Medicine, University of Leipzig, Leipzig, Germany, **2** Department of Neurosurgery, Paracelsus Hospital Zwickau, Zwickau, Germany

‡ These authors are joint senior authors on this work.
* marina.bigl@medizin.uni-leipzig.de (MB); nicole.scholz@medizin.uni-leipzig.de (NS)

Citation: Heydasch U, Kessler R, Warnke J-P, Eschrich K, Scholz N, Bigl M (2021) Functional diversity of PFKFB3 splice variants in glioblastomas. PLoS ONE 16(7): e0241092. https://doi.org/10.1371/journal.pone.0241092

Editor: Klaus Roemer, Universitat des Saarlandes, GERMANY

Received: October 2, 2020

Accepted: June 8, 2021

Published: July 7, 2021

Data Availability Statement: All relevant data are within the manuscript and its Supporting information files.

Funding: This work was supported by a grant from the Wilhelm-Sander Stiftung to RK (2004.010.1; https://www.wilhelm-sander-stiftung.de) and by grant from the Deutsche Forschungsgemeinschaft to NS (265903901, FOR2149 P01 [SCHO1791/1-2]; https://www.dfg.de).

Competing interests: The authors have declared that no competing interests exist.

Abstract

Tumor cells tend to metabolize glucose through aerobic glycolysis instead of oxidative phosphorylation in mitochondria. One of the rate limiting enzymes of glycolysis is 6-phosphofructo-1-kinase, which is allosterically activated by fructose 2,6-bisphosphate which in turn is produced by 6-phosphofructo-2-kinase/fructose-2,6-bisphosphatase (PFK-2/FBPase-2 or PFKFB). Mounting evidence suggests that cancerous tissues overexpress the PFKFB isoenzyme, PFKFB3, being causing enhanced proliferation of cancer cells. Initially, six PFKFB3 splice variants with different C-termini have been documented in humans. More recently, additional splice variants with varying N-termini were discovered the functions of which are to be uncovered. Glioblastoma is one of the deadliest forms of brain tumors. Up to now, the role of PFKFB3 splice variants in the progression and prognosis of glioblastomas is only partially understood. In this study, we first re-categorized the PFKFB3 splice variant repertoire to simplify the denomination. We investigated the impact of increased and decreased levels of PFKFB3-4 (former UBI2K4) and PFKFB3-5 (former variant 5) on the viability and proliferation rate of glioblastoma U87 and HEK-293 cells. The simultaneous knock-down of PFKFB3-4 and PFKFB3-5 led to a decrease in viability and proliferation of U87 and HEK-293 cells as well as a reduction in HEK-293 cell colony formation. Overexpression of PFKFB3-4 but not PFKFB3-5 resulted in increased cell viability and proliferation. This finding contrasts with the common notion that overexpression of PFKFB3 enhances tumor growth, but instead suggests splice variant-specific effects of PFKFB3, apparently with opposing effects on cell behaviour. Strikingly, in line with this result, we found that in human IDH-wildtype glioblastomas, the *PFKFB3-4* to *PFKFB3-5* ratio was significantly shifted towards *PFKFB3-4* when compared to control brain samples. Our findings indicate that the expression level of distinct PFKFB3 splice variants impinges on tumorigenic properties of glioblastomas and that splice pattern may be of important diagnostic value for glioblastoma.

Introduction

Glioblastoma is the most common malignant primary tumor in brain. The high rate of aerobic glycolytic flux, a mechanism known as the Warburg effect, is a metabolic hallmark of tumors including glioblastoma [1]. As a result, glioblastoma cells possess increased levels of fructose-2,6-bisphosphate (F2,6BP), the main regulator of 6-phosphofructo-1-kinase, which in turn represents one of the rate-controlling glycolytic enzymes [2, 3]. Both synthesis and degradation of F2,6BP are catalysed by 6-phosphofructo-2-kinase/fructose-2,6-bisphosphatase (PFK-2/FBPase-2, in human PFKFB, EC 2.7.1.105/EC 3.1.3.46), which belongs to a family of homodimeric bifunctional enzymes [4]. In human, there are four major PFKFB isoenzymes encoded by four genes (*PFKFB1-4*), which possess high sequence homologies within their catalytic core domains. PFKFB isoenzymes differ in pattern and level of expression as well as in functional properties including their response to protein kinases [5]. Typically, PFKFBs have a similar capacity to function as kinase and bisphosphatase. However, for PFKFB3 this balance has been shown to be shifted towards kinase activity, which in turn enables sustained high glycolysis rates [6]. *PFKFB3* gene is localized on chromosome 10p15.1 [7] and is ubiquitously distributed throughout human tissues. It shows elevated levels in rapidly proliferating cells such as tumorigenic and leukemic cells [8]. Both inflammatory and hypoxic stimuli were shown to trigger PFKFB3 expression [9, 10]. Consistently, *PFKFB3* contains multiple copies of the oncogene-like AUUUA instability element within its 3′ untranslated region [7]. Moreover, PFKFB3 was found to be shuttled to the nucleus by a process which appears to be triggered by a highly conserved nuclear localization motif within the C-terminus [11]. F2,6BP synthesized in the cell nucleus increases cyclin-dependent kinase (CDK)–dependent phosphorylation of the CIP/KIP-protein p27, which is subsequently degraded in the proteasome [12]. PFKFB3 was also reported to participate in G2/M transition [13] and to regulate the cell cycle (transition from G1 to S phase) by binding to cyclin dependent kinase 4 (CDK4) [14]. PFKFB3 was identified as a critical factor in homologous recombination repair of DNA double-strand breaks [15]. Conclusively, PFKFB3 constitutes a metabolic key player, which causally couples cell cycle and glucose metabolism to proliferation of cancer cells [16]. In humans, six PFKFB3 splice variants (designated UBI2K1-6) have been described [17]. The diversity of these transcripts results from a combination of different exons encoding varying PFKFB3 C-termini (Fig 1). Splice variant UBI2K5 and its role in cancer metabolism was studied in detail [18, 19], but thus far the role of most other splice variants remains enigmatic. Increased expression levels of total *PFKFB3* in high-grade astrocytomas compared to low-grade astrocytomas and non-neoplastic brain tissue were found [20]. Healthy brains express the entire set of *PFKFB3* splice variants (*UBI2K1-6*). In contrast, glioblastoma predominantly express *UBI2K4-6* with *UBI2K5* and *UBI2K4* being increased and decreased respectively compared to tissue from control brains [21]. Based on this inverse correlation between *UBI2K4* expression and the growth rate of cells, it was concluded that *UBI2K4* suppresses tumor cell growth [21]. To elucidate the impact of UBI2K4 on the metabolism of cancer cells in detail we analyzed UBI2K4 deficient HEK-293 and a glioblastoma cell line (U87) with respect to their viability and proliferation capabilities.

In the past, the denomination of different PFKFB3 splice variants differed across laboratories. As a result, identical isoforms are often non-uniformly referenced. For example, the predominant splice variant in human brain (UBI2K5) is referred to as the ubiquitous PFK-2/FBPase-2 [22], placenta PFK-2/FBPase-2 [23] 'Progestin Responsive Gene 1' [24] and PFKFB3-ACG [18] despite identical amino acid sequences of the respective proteins. Similarly, UBI2K4 and inducible PFK-2 (iPFK-2) [25] refer to the same molecule. To confuse matters even more, recently NCBI-PubMed published additional PFKFB3 splice variants designated 'variant 1–8 and also putative splice variants designated as X2-X8'. Two of them are synonyms

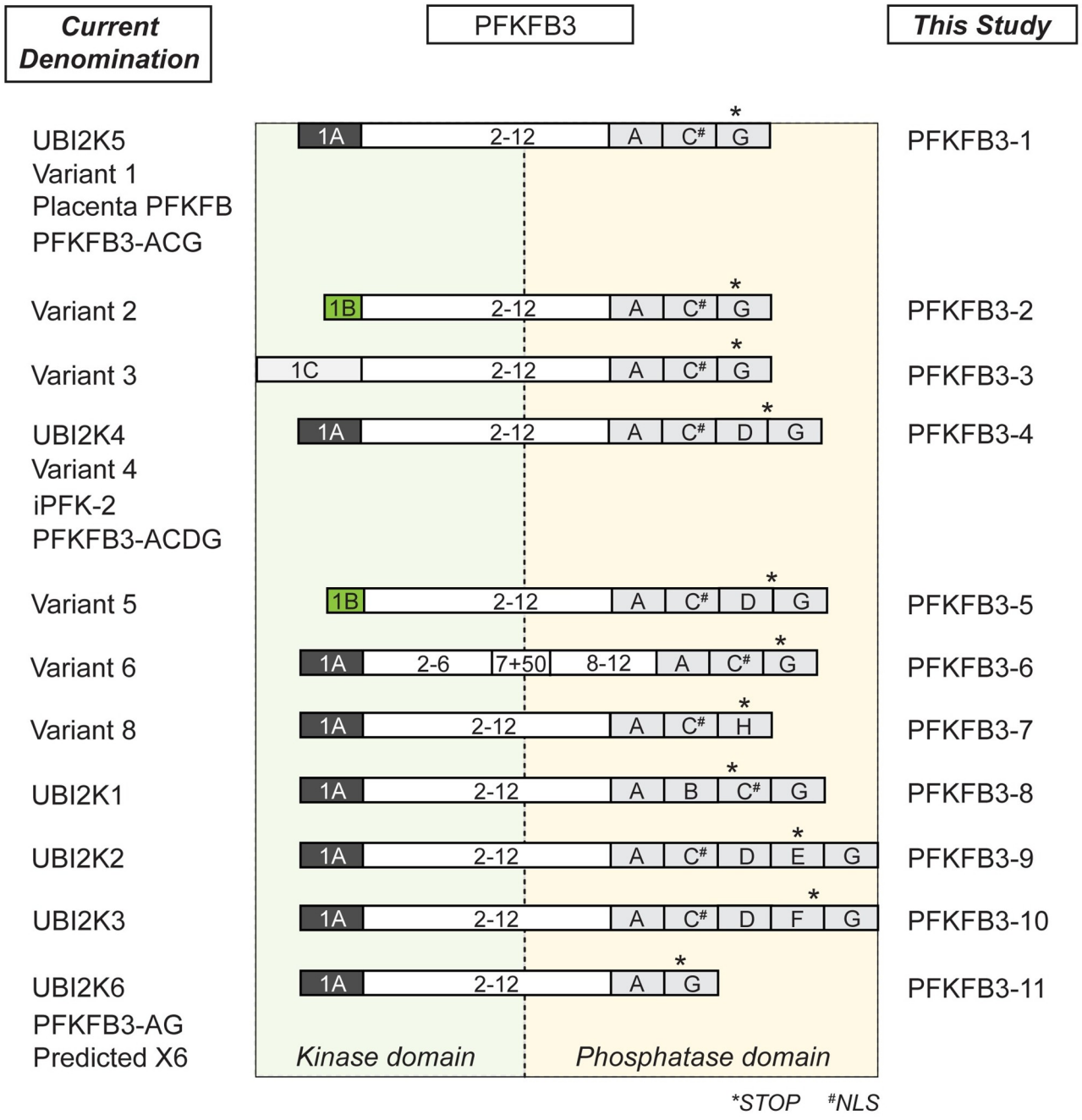

Fig 1. Schematic illustration of the transcript repertoire generated from the human *PFKFB3* gene locus. Scheme based on sequence analyses carried out using Basic Local Alignment Search Tool (BLAST) and Multalin interface page (multalin.toulouse.inra.fr/multalin). Left panel shows the current denomination of splice variants documented in the literature and NCBI database; right panel indicates the denomination PFKFB3-1-11 used in this study. Conserved exons are depicted as white boxes with numbers except for PFKFB3-6, which contains an additional insert of 50 bp in exon 7. Variable N-terminal and C-terminal exons are colored and indicated by capital letters. * indicates stop codon of each splice variant, # indicates predicted nuclear localization signals (NLS). PFKFB3-1: NM_004566.4 [17, 18, 22–24]; PFKFB3-2: NM_001145443.3; PFKFB3-3: NM_001282630.3; PFKFB3-4: NM_001314063.2 [17, 18, 25]; PFKFB3-5: NM_001323016.2; PFKFB3-6: NM_001323017.2; PFKFB3-7: NM_001363545.2; PFKFB3-8: AJ272438.1 [17]; PFKFB3-9: AJ295747.1 [17]); PFKFB3-10: AJ272439.1; PFKFB3-11: AJ272440.1 [17, 18], XM_005252464.2; Variant 7: NR_1365554.2 represents non-coding RNA and is therefore not shown.

https://doi.org/10.1371/journal.pone.0241092.g001

for previously described splice variants UBI2K4 (variant 4) and UBI2K5 (variant 1) and also the putative splice variant X6 is synonymous for UBI2K6. Variant 5 closely resembles UBI2K4 (variant 4), however, both differ in their N-termini. The present paper focuses on investigating in detail the impact of UBI2K4 (variant 4) and variant 5 on the metabolism of glioblastoma cells. Thus, to unambiguously refer to particular splice variants in this study we utilize a straight-forward PFKFB3 nomenclature with numbers referencing isoenzyme and splice variants (Fig 1). Therefore, variant 4 (UBI2K4) and variant 5 are designated as PFKFB3-4 and PFKFB3-5.

In this paper, we report a decreased viability and proliferation rate of PFKFB3-4 and PFKFB3-5-deficient U87 and HEK-293 cells, which was accompanied by a reduction in colony formation. Overexpression of PFKFB3-4 but not PFKFB3-5 resulted in increased cell viability and proliferation. In IDH-wildtype glioblastomas, the ratio of *PFKFB3-4* to *PFKFB3-5* was significantly shifted towards *PFKFB3-4* compared to control brain samples. Our findings indicate different roles for splice variants PFKFB3-4 and PFKFB3-5 in healthy as well as malignant cells and implicate an important diagnostic role of these specific PFKFB3 splice variants in glioblastomas.

Materials and methods

Sample collection and genotyping

The study included 30 isocitrate dehydrogenase (IDH) -wildtype glioblastomas of World Health Organization grade IV, which were diagnosed as primary glioblastomas without clinical history. The glioblastomas were resected from patients undergoing neurosurgery at the Department of Neurosurgery, Paracelsus Hospital Zwickau (Germany). Written consent of each patient was obtained to collect the tissue for research purposes.

Histopathological and molecular diagnosis were done by K. Petrow (Institute of Pathology, Zwickau, Germany) and C. Mawrin (Department of Neuropathology, Otto-von-Guericke University, Magdeburg) based on the World Health Organization Classification [26]. The 15 surgical specimens of tumor-adjacent, macroscopically normal brain tissues according to criteria thoroughly described, were used as controls (S1 Table). The ethics committee of the University of Leipzig approved this study (Reg. No. 167-14-02062014).

Genomic DNA of tumor samples was screened for IDH1 and IDH2 mutations as previously described Hartmann [27]. To analyze the IDH1 locus we used primers IDH1f and IDH1r, for IDH2 we used IDH2f and IDH2r (S2 Table). Primers used in this study were synthesized by Metabion (Martinsried, Germany).

Unless stated otherwise, PCR products and plasmids generated in this study were sequenced using the BigDye Terminator Cycle Sequencing Kit and the Applied Biosystems 3130xl Genetic Analyzer (Applied Biosystems, Weiterstadt, Germany).

Cell culture

The following cell lines were used: HEK-293 (ATCC CRL-1573); U87-glioblastoma cell line (ATCC HTB-14); SH-SY5Y (ATCC CRL-2266); 1321N1 human astrocytoma cell line (ECACC 86030402); LN-405 glioblastoma cell line (ACC 189). All cell cultures were maintained at 37˚C in humidified atmosphere containing 5% CO_2 and grown as monolayers in DMEM (Biochrom, Berlin, Germany), supplemented with 4.5 g/l glucose, 10% fetal bovine serum (Hyclone, Bonn, Germany), 1% penicillin/streptomycin/neomycin (Invitrogen, Karlsruhe, Germany). U87 and SH-SY5Y cells were grown in DMEM additionally supplemented with 1% non-essential amino acids (Invitrogen, Karlsruhe, Germany).

RNA and protein isolation

Total RNA and protein from tissue and cell culture samples were extracted using TRIzol according to the manufacturer's protocols (Invitrogen, Karlsruhe, Germany). Concentration and quality of RNA were determined by spectrophotometry using the NanoDrop® ND-1000 (PeqLab, Erlangen, Germany). Total protein content was measured using the BioRad DC protein assay kit (Munich, Germany).

Construction of shRNA-encoding plasmids for PFKFB3-4+5 silencing

Human *PFKFB3-4+5* specific shRNA was designed as a 63-mer containing a hairpin-loop, which was cloned into H1 RNA polymerase promoter-containing pSuper vector. The vector contains an inducible system to stably integrate siRNA and an EGFP cassette [28]. A Zeocin resistance cassette was used to select stably transfected cells.

For siRNA experiments, an overlapping sequence-fragment between exon D and G (Fig 2A) in the C-terminus of *PFKFB-4* and *PFKFB-5* was used. The *shPFKFB3-4+5*-coding sequences and sh-scrambled sequences are listed in S2 Table. As judged from BLAST search scr-shRNAs show no significant sequence similarity to mouse, rat, or human gene sequences. The oligonucleotides were annealed and subcloned downstream of the H1 promoter into pTER-EGFP using *Hind*III and *Bgl*II. The RNAi sequence for shRNA was identical to that of siRNA (S2 and S3 Tables).

Engineering of PFKFB3-4 and PFKFB3-5 overexpression plasmids

Total RNA was obtained from astrocytoma cell line 1321N1 using TRIzol and reverse-transcribed with Transcriptor Reverse Transcriptase according to the manufacturer's instructions (Roche Diagnostics, Mannheim, Germany). Full-length human *PFKFB3-4* was generated by standard PCR using primers PFKFB3-4 reverse and PFKFB3-4 forward (S2 Table). The resulting amplicon was cloned into pcDNA3.1/Hygromycin plasmid vector (Invitrogen, Waltham, MA, USA) using *Apa*I and *Afl*II. Similarly, the full-length fragment of human *PFKFB3-5* was amplified with primers PFKFB3-5 reverse and PFKFB3-5 forward and subcloned into the plasmid pGEM-T using the T/A Cloning Kit (Promega, Mannheim, Germany). Subsequently, the amplicon was digested with Xba*I* and Hind*III* and inserted into the pcDNA3.1/Hygromycin plasmid vector (Invitrogen, Waltham, MA, USA). After confirmation by sequencing and enzymatic digest, both constructs were assigned the names pcDNA-PFKFB3-4 and pcDNA-PFKFB3-5.

Generation of stable cell lines

Transfection of plasmids for overexpression purposes was performed using X-tremeGENE™ HP (Roche Diagnostics) according to the manufacturer's instructions. To generate stably-expressing HEK-293 and U87 cell lines 150 μg/ml hygromycin B (Invitrogen) was added to the medium. Individual hygromycin-resistant colonies were selected and expanded.

Transfection of plasmids for knockdown purposes (shRNA-vectors) was performed using FuGene®HD (Roche Diagnostics) according to the manufacturer's instructions. To generate stable cell lines the transfected cells were selected with Zeocin (200 μg/ml, Invitrogen, Waltham, MA, USA) and by EGFP fluorescence.

Transient overexpression of PFKFB3-5

Transient transfection of plasmids for overexpression purposes was performed using X-tremeGENE™ HP (Roche Diagnostics) according to manufacturer's instructions. The cells were

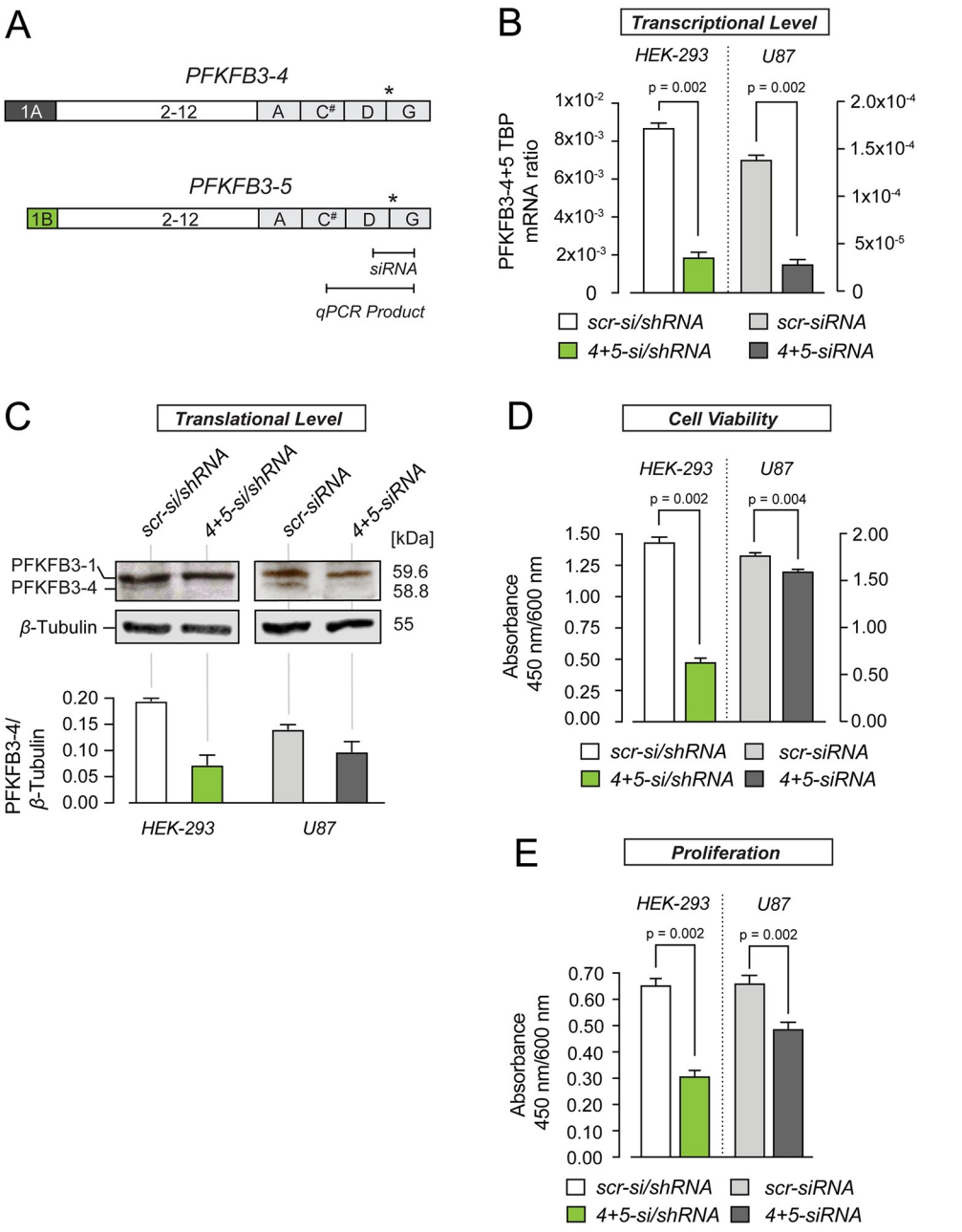

Fig 2. Knock-down of PFKFB3-4+5 alters proliferation and viability of HEK-293 and U87 cells. (A) Schematic representation of PFKFB3-4 and -5 with indication of PCR/qPCR as well as siRNA target sequences. Note that PFKFB3-4 and -5 differ in their N- but not C-termini. * indicates the stop codon, # indicates the predicted nuclear localization signal (NLS). siRNA probes used for gene silencing recognize sequences between exons D and G, in PFKFB3-4 and PFKFB3-5. (B) Quantification of stably and transiently inhibited *PFKFB3-4+5* expression in HEK-293 and transiently inhibited *PFKFB3-4+5* in U87 cells, respectively. The RNAi sequence for siRNA was identical to that of shRNA. mRNA levels in cells transfected with *PFKFB3-4+5* si/shRNA was compared to scr-si/shRNA-transfected cells. mRNAs were detected 24 h after siRNA treatment. *PFKFB3-4+5* expression was normalized to the amount of TBP mRNA measured by quantitative PCR. mRNA-based experiments were done as duplicates in 3 independent experiments (N = 3, n = 2). The values represent the mean ± SEM. (C) Western blot analysis of PFKFB3 protein expression following si/shRNA mediated PFKFB3-4+5 knock-down utilizing polyclonal PFKFB3 antibody. Proteins were detected 48 hours after siRNA treatment. *β*-Tubulin served as loading control. 30 μg protein/lane was applied. Western blot shows the 58.8 kDa band in scr-si/shRNA cells. The ratio of protein bands (PFKFB3-4/5 to *β*-Tubulin) was calculated from the intensity values of protein bands (n = 3). (D) Quantification of cell viability of PFKFB3-4 +5-depleted HEK-293 and U87 cells compared to scr-si/shRNA treated cells via WST-1 assay. After a 4 h incubation

period with WST-1 reagent the absorbance was measured. The experiments were run as duplicates in three independent experiments (N = 3, n = 2). The values represent the mean ± SEM. (E) Quantification of cell proliferation of PFKFB3-4+5-depleted HEK-293 and U87 cells compared to scr-si/shRNA treated cells via BrdU-test. After 20 h incubation period with BrdU, the absorbance was measured at 450 nm/600 nm. BrdU tests were done as duplicate in 3 independent experiments (N = 3, n = 2). Values represent the mean ± SEM. All groups were compared using the Mann Whitney test.

https://doi.org/10.1371/journal.pone.0241092.g002

harvested 24–48 h after transfection. mRNA was measured 24 h after transfection and protein was measured 48 h after transfection.

Knockdown in HEK-293 and U87 cells

For transient depletion of PFKFB3-4 and PFKFB3-5 in U87 cells, duplex siRNA was obtained from Thermo Fisher Scientific Biosciences (St. Leon-Rot, Germany) with UU overhangs (standard). Sequences are listed in S3 Table.

Transfection for transient knockdown purposes (siRNA) was performed using DharmaFECT™ transfection reagents (Thermo Fisher Scientific) according to the manufacturer's protocol. The transfection reagents were used with a final siRNA concentration of 25 nM. The cells were harvested 24–48 h after transfection (mRNA: 24 h, protein: 48 h).

In order to measure cell viability and proliferation stably transfected HEK-293 cells with shRNA-vectors were additionally transfected with duplex siRNA to knockdown *PFKFB3-4* and *PFKFB3-5* in HEK-293 cells. Procedure was carried out as for U87 cells. To measure cell growth and colony formation of HEK-293 cells under PFKFB3-4 + 5-deficient condition, only shRNA was used.

qPCR

For quantitative PCR, 500 ng of total RNA were reverse-transcribed using Transcriptor Reverse Transcriptase (Roche Diagnostics) and oligo-d$(T)_{n = 18}$ primer (Metabion) according to the manufacturer´s protocol. For quantification of PFKFB3-4+5, the cDNA was amplified in a LightCycler (Roche Diagnostics) using primers 3PFK2fo2 and iPFK2re6 as well as the LightCycler FastStart DNA Master Plus Set SYBR Green I Kit (Roche Diagnostics) according to the instruction manual.

To reliably calculate the RNA concentration, we generated RNA standards. To this end, a specific *PFKFB3-4+5* fragment (Fig 2A) was reverse transcribed from total RNA of human brain (S1 Table, Pat.-No. 104) and PCR-amplified using primers 3PFK2fo2 and iPFK2re6 (S2 Table). The PCR product was cloned into the pGEM-T vector. Sense strand RNA was transcribed using the Megascript *in vitro* Transcription Kit (Ambion, Wiesbaden, Germany) according to the manufacturer's instructions to yield standard RNA. Standard curves were generated during each RT-PCR by serial fivefold dilution as previously described [21].

The TATA box binding protein (TBP) standard synthesis and the TBP quantification were carried out with primers TBPfo and TBPre. *PFKFB-1* and *PFKFB-11* were quantified as above with the primer pairs iPFK2Fo/PFK2Re and HBF10/6PFK2re5, respectively (S2 Table). RNA standards for *PFKFB-1* and *PFKFB-11* were synthesized as described for *PFKFB3-4+5*.

Multiplex PCR

To pinpoint differences in the expression of *PFKFB3-4* and *PFKFB3-5*, a multiplex PCR was established using *PFKFB3-4* and *PFKFB3-5* specific forward primers 4_Fo and 5_Fo as well as reverse primer 4/5_Re (S2 Table), which anneals to both splice variants (Fig 7A). 500 ng total

RNA were reverse-transcribed with Transcriptor Reverse Transcriptase (Roche Diagnostics) using the primer 4/5_Re. PCR was performed using a master mix including the Expand high fidelity Taq polymerase (Roche Diagnostics). Amplicons were analyzed by standard agarose gel-electrophoresis. The ratio of PCR fragments was calculated from the intensity values of DNA bands analyzed with Herolab E.A.S.Y Plus Video gel documentation system (Herolab, Wiesloch, Germany).

To estimate the sensitivity of the primer pairs in the multiplex system, standard curves were established and the efficiency of the PCR was tested. The standard RNAs were synthesized from both target cDNA, which were subcloned in pGEM-T by an *in vitro* RNA synthesis kit (MAXIscript; Ambion). The copy numbers of RNA molecules were calculated on the basis of their absorbance values. The RNA products were serially diluted to prepare standard RNA solutions and were subjected to RT-PCR as described above.

Western blotting

5–30 μg protein per lane were separated by standard SDS-PAGE (7,5% acrylamide gel) and semi-dry blotted onto nitrocellulose membranes (PALL Life Sciences, Dreieich, Germany). The membranes were blocked with 5% skimmed milk in Tris-buffered saline Tween 20 (TBST) for 2 h. The membranes were incubated with primary antibodies: rabbit-anti-human PFKFB3 (1:1000; overnight; 4˚C; ABIN 392768, Abgent/Biomol, Hamburg) and mouse-anti-β-Tubulin Antibody (1:5000; 1h, RT, E7, DSHB, Iowa, USA). Secondary antibody was incubated for 1 h at 25˚C with donkey-anti-rabbit IgG POD (1:30000, Dianova, Hamburg), IRDye 680RD goat-α-rabbit (1: 15000; Li-COR, Nebraska, USA) or goat-anti-mouse IRDye 800CW (1:15000; Li-COR, Nebraska, USA). For the blots for si/shRNA experiments and for the overexpression of PFKFB3-4, the incubation of the PFKFB3 antibody and of anti-ß-tubulin antibody was carried out one after the other. To investigate the overexpression of PFKFB3-5, PFKFB3 and β-tubulin antibodies were incubated at the same time.

After each antibody incubation step the membrane was washed 3 x 5 min with TBST. Visualisation of PFKFB3 proteins under knockdown conditions and overexpression of PFKFB3-4 was done using an enhanced chemiluminescence kit (SuperSignal West Dura, Thermo Fisher Scientific).

Visualization of overexpressed PFKFB3-5 as well as β-Tubulin (served as loading control) was carried out using the Odyssey FC 2800 (Li-COR Biosciences, Bad Homburg, Germany).

The ratio of protein bands (PFKFB3-4/5 to β-Tubulin) was calculated from the intensity values of protein bands analyzed with Herolab E.A.S.Y Plus Video gel documentation system (Herolab, Wiesloch, Germany).

Cell viability and cell proliferation

Cell viability was evaluated using the colorimetric WST-1 assay (Roche Diagnostics). After a 4-h incubation period with WST-1 reagent the absorbance was measured at 450 nm/ 600 nm using a microplate reader (ELISA-Reader Zenyth 200st, Anthos, Krefeld, Germany).

Cell proliferation was evaluated using a colorimetric bromodeoxyuridine (BrdU) cell proliferation ELISA kit (Roche Diagnostics). After 20-h incubation period with BrdU, the absorbance was measured at 450 nm/600 nm using a microplate reader (ELISA-Reader Zenyth 200st).

Cell growth and anchorage independent growth

To generate growth curves, PFKFB3-4+5-deficient and src-shRNA HEK-293 cells were seeded (5000 cells/12-well) and every 24 h cells were counted until confluency was reached.

Anchorage independent growth was investigated using a soft-agar test. A total of 5000 cells per 6-well were resuspended in 0.4% agarose in DMEM and were plated on top of a 0.6% bottom agarose DMEM layer. The medium was replenished every 2 d. After 14 d, colonies were counted in five randomly selected fields per well under x10 magnification.

Statistics

Data were analyzed with GraphPad Prism software (version 8.0, La Jolla, CA). Group means were compared by a two-tailed Student's t-test, unless the assumption of normality of the sample distribution was violated. In this case group means were compared by a non-parametric rank sum test (Mann Whitney-Test). Data are reported as mean ± SEM, n indicates the sample number (e.g. duplicates or triplicates), N indicates the number of individual experiments and p denotes the p-value.

Results

General considerations

Previously, we have shown that the *PFKFB3* splice pattern is notably different between healthy brain tissue and rapidly proliferating malignant gliomas [20]. We found that *PFKFB3-1* (UBI2K5) mRNA concentration was elevated in high grade astrocytomas (not published), whereas *PFKFB3-4* (UBI2K4) mRNA expression level was decreased when compared to normal brain tissue [21]. Importantly, the quantitation of *PFKFB-4* mRNA involved the recently detected *PFKFB3-5* (PFKFB3 splice variant 5) because the C-termini of PFKFB3-4 and PFKFB3-5, which harbor the phosphatase activity, are structurally identical, whereas their N-terminal ends, which accommodate the kinase activity, are different (Fig 1).

To gain more detailed insight about the role of PFKFB3-4 and PFKFB3-5 in glioblastomas, we employed the U87 glioblastoma cell line and investigated the knockdown and overexpression of these splice variants in relation to viability and proliferative capacity of U87 cells as a read out. In parallel, we studied these aspects in non-glial HEK-293 cells, as their PFKFB3 splice patterns for PFKFB3-4 and PFKFB3-5 are similar to that of healthy brain tissue (Fig 7A).

Knockdown of PFKFB3-4+5 reduces proliferation and cell viability

We used RNA interference (RNAi) to reduce the *PFKFB3-4+5* expression in both HEK-293 cells (stable and transient knockdown) and U87 cells (transient knockdown) (Fig 2A). The selective inhibition of PFKFB3-4 and PFKFB3-5 was not possible because the variable exons 1A, 1B and D also occur in several other splice variants. First, we measured the transcript quantity of *PFKFB3-4+5* in cells stably and transiently transfected (HEK-293 cells) and transiently transfected (U87) with PFKFB3-4+5 siRNA next to control cells expressing the respective scr-si/shRNA (Fig 2B). Using shRNA and additional siRNA for HEK-293 cells had a greater knockdown effect. Establishing stable shRNA for U87 cells was not possible.

As expected both stable and transient knockdown in HEK-293 and U87 cells with PFKFB3-4+5 si/shRNA showed a significant reduction of *PFKFB3-4+5* transcripts compared to scr-si/shRNA cells. The *PFKFB3-4+5* mRNA level in control HEK-293 cells, was higher than in U87 cells. The decrease in *PFKFB3-4+5* mRNA induced by the knockdown was stronger in HEK-293 (from $8.5^{*}10^{-3}$ to $1,7^{*}10^{-4}$ PFKFB3-4+5/ TBP mRNA ratio) than in U87 cells (from $2^{*}10^{-3}$ to $2^{*}10^{-5}$ PFKFB3-4+5/ TBP mRNA ratio). The sequence of siRNA and shRNA probes was identical.

Consistently, western blot analysis of protein extracts from these cells showed reduced levels of PFKFB3-4 (Fig 2C, S1 and S2 Appendices). Notably, PFKFB3-5 protein seems to be

expressed in very low copy number and was not detectable in our hands. To determine whether the decreased expression of PFKFB3-4+5 has an effect on proliferation and/or cell viability of HEK-293 and U87 cells, we performed WST and BrdU assays quantifying the metabolic activity and DNA replication rates of cells, respectively (Fig 2D and 2E). In both cell lines, knockdown of PFKFB3-4+5 resulted in decreased cell viability and proliferation compared to control cells. Interestingly, the effect appeared more pronounced in HEK-293 cells (Fig 2D). Conceivably, different mRNA levels for *PFKFB3-4+5* in both cell lines are responsible for the higher growth inhibition after knockdown of *PFKFB3-4+5* in HEK-293 cells as compared to U87 cells. Additionally. the different transfection methods used in HEK-293 and U87 cells also account for the differential effects on cell viability (Fig 2D).

Knockdown of PFKFB3-4+5 impinges on cell growth and colony formation

To analyze whether the reduction of PFKFB3-4 and -5 affects the cell number, we quantified stably transfected PFKFB3-4+5 shRNA HEK-293 cells for a period of five days. Similar cell numbers were counted in PFKFB3-4+5-deficient and control samples over a period of the first four days. Interestingly, after five days knock-down of PFKFB3-4+5, a significant reduction of cell number compared to control was observed (Fig 3A and 3B, S3 Appendix). Moreover, as glioma cells have the capacity to grow three-dimensionally through neuronal tissues, we sought to interrogate the behaviour of PFKFB3-4+5-deficient HEK-293 cells in soft agar by observing colony formation. Cell colony number dropped by 15% after 14 days, which may mirror the reduction of the malignant facility of these cells (Fig 3C and 3D, S4 Appendix). As we used for this experiments shRNA treated HEK-293 cells without additional siRNA treatment, the effects on cell growth were lower.

Overexpression of PFKFB3-4 and PFKFB3-5 causes opposite effects on cell viability and proliferation

Previously, overexpression of variant PFKFB3-4 C-terminally appended with a biochemical tag (Flag-tag) was shown to reduce both cell viability and anchorage-independent growth of U87 cells [21]. The C-terminal region of PFKFB3-4 encodes the phosphatase moiety of PFKFB3. Hence, it is conceivable that fusion of any tag to this region will disturb the phosphatase function, which in turn may be responsible for these cellular changes. Based on RNAi-mediated effects documented in this study, we hypothesized that overexpression of PFKFB3-4 would lead to an increase in cell viability and proliferation. To test this, we stably overexpressed PFKFB3-4 in HEK-293 and U87 cells. Fig 4A and 4B (S5 and S6 Appendices) show a significant increase of this PFKFB3 variant on transcriptional (increase by more than 10 times) and translational levels (increase by 400 times in HEK-293 cells and over 3 times in U87 cells). Indeed, we found that elevated levels of PFKFB3-4 affected proliferation and cell viability positively (Fig 4C and 4D). But overexpression of PFKFB3-4 did not influence mRNA levels of *PFKFB3-1* and *PFKFB3-11*, splice variants which are constitutively expressed in glioblastoma cells (Fig 4E).

In a separate set of experiments, we tested the effects of PFKFB3-5 on these cellular parameters. We followed the same rationale. First, we analysed the transient overexpression of PFKFB3-5 in HEK-293 and U87 cells via qPCR and Western blot analysis (Fig 5A and 5B, S7 and S8 Appendices). Transient overexpression resulted in an increase of mRNA of *PFKFB3-5* 3600 times in HEK-293 and 12500 times in U87 cells, protein is increased 450 times in HEK-293 cells and 70 times in U87 cells. Interestingly, despite the high levels of PFKFB3-5 due to transient overexpression, cell viability and proliferation remained indistinguishable from controls (Fig 5C and 5D). For this reason, we asked if overexpression of PFKFB3-5 influences the

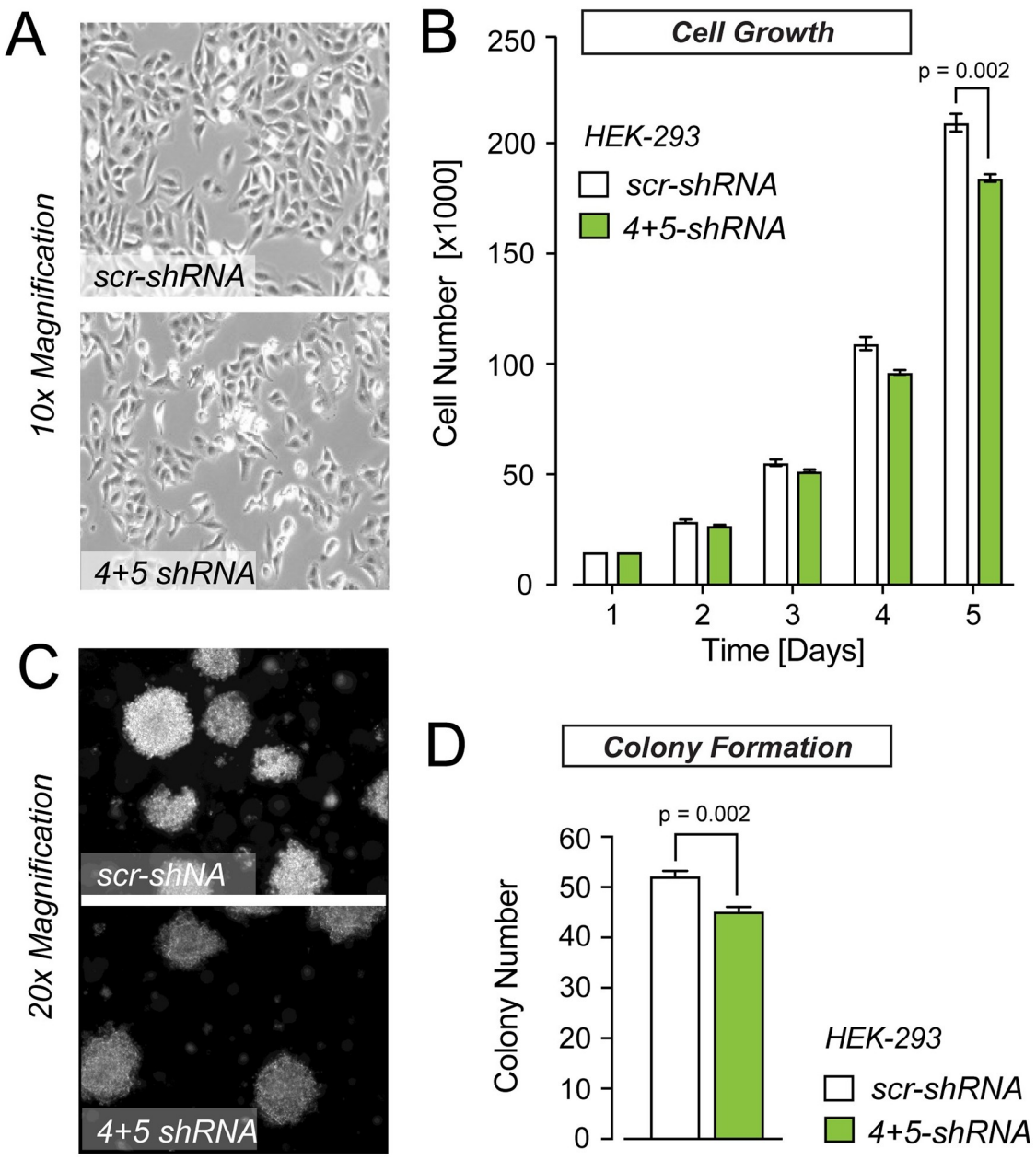

Fig 3. PFKFB3-4+5 knockdown leads to decreased cell growth and colony formation. (A) Representative brightfield image of scr-shRNA (upper panel) and 4+5 shRNA treated (lower panel) HEK-293 cells cultured in 12-well plates. Image was taken after five days of cell seeding. (B) Quantification of cell growth of HEK-293 cells with stably reduced levels of PFKFB3-4+5 compared to cells expressing scr-shRNA. 5000 cells/12-well for each condition. The colony numbers are the mean ± SEM. The cell growth experiment was done as duplicate determinations with three independent experiments (N = 3, n = 2). The cell number was quantified by cell counting in 12-well plates every 24 hours until approximately 80% confluency was reached. All groups were compared using the Mann Whitney test. (C) Representative images of soft agar colonies formed by HEK-293 cells (scr-shRNA) and HEK-293 cells with stably reduced PFKFB3-4+5 levels (4/5 shRNA). The cells (5000 cells) were cultured for 14 d in 6-well plates on soft agar. (D) Quantification of HEK-293 cell colonies from (C) after 14 d in culture. The colony formation was quantified in three independent experiments as duplicates (N = 3, n = 2). The numbers are the mean ± SEM. The groups were compared using Mann Whitney test.

https://doi.org/10.1371/journal.pone.0241092.g003

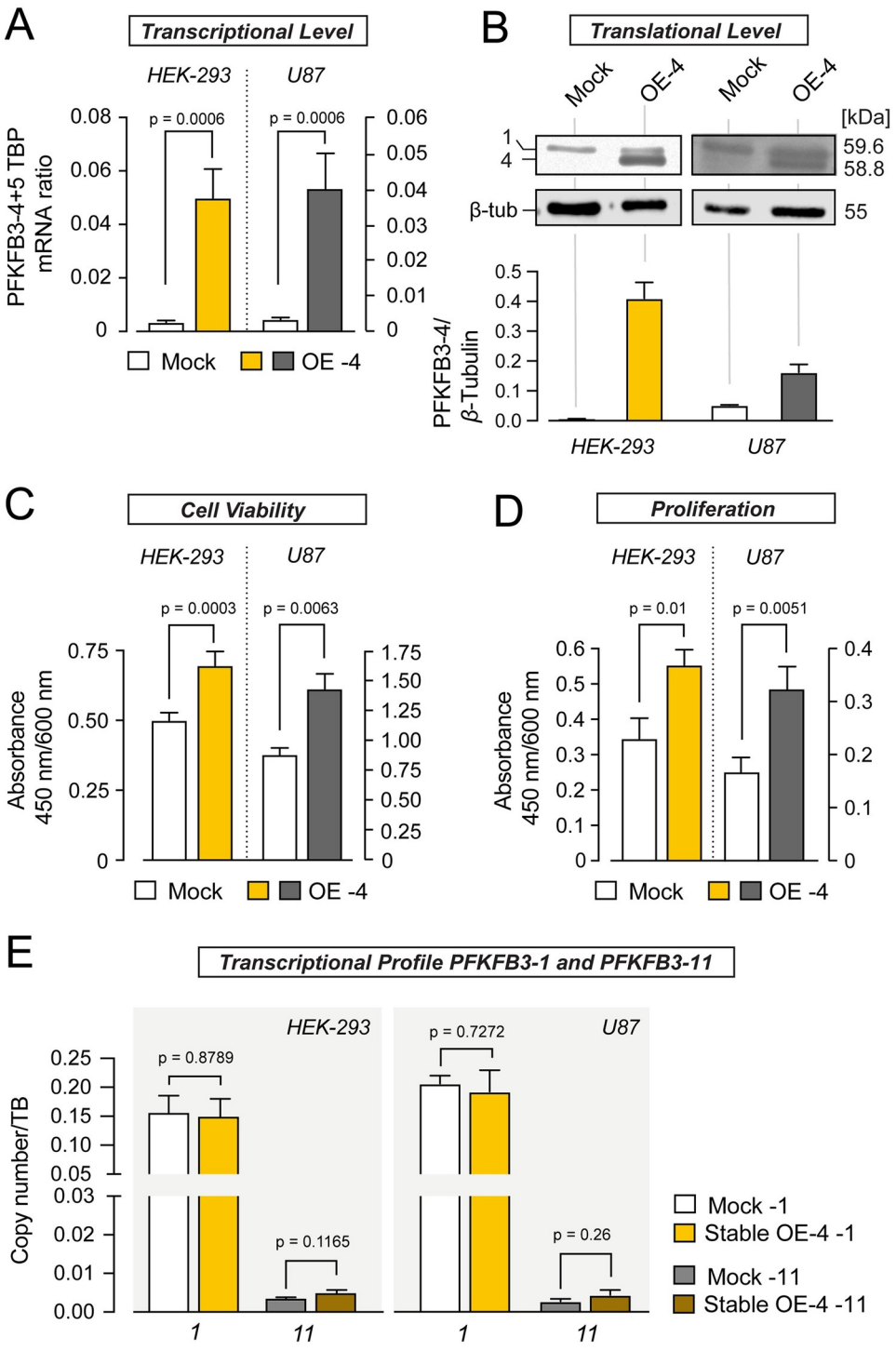

Fig 4. PFKFB3-4 overexpression facilitates cell viability and proliferation. (A) Quantification of *PFKFB3-4+5* mRNA levels from HEK-293 (yellow) and U87 cells (grey) stably overexpressing *PFKFB3-4* (OE -4), respectively. mRNA-measurement was done with 4 independent experiments (N = 4, n = 1–2). *PFKFB3-4* mRNA quantity measured by quantitative PCR was normalized to the amount of TBP mRNA and compared to mock samples. (B) Western blot analysis to confirm the overexpression of PFKFB3-4 with polyclonal PFKFB3 antibody. *β*-Tubulin served as loading control, 10 μg protein was loaded per lane. 1 refers to PFKFB3-1 and 4 refers to PFKFB3-4. The ratio of protein bands (PFKFB3-4 to *β*-Tubulin) was calculated from the intensity values of protein bands (n = 3). (C) Effect of stable PFKFB3-4 overexpression on cell viability, measured by WST-1 assay. After a 4 h incubation period with WST-1 reagent the absorbance was measured at 450 nm/600 nm. WST-test was done in 4–5 independent experiments in 7–8

times analyses (N = 4–5, n = 7–8). (D) Effect of stable PFKFB3-4 overexpression on proliferation measured by BrdU-assay. After 20 h incubation period with BrdU, the absorbance was measured at 450 nm/ 600 nm. BrdU-test were done three times in 6–7 analysis (N = 3, n = 6–7). (E) Influence of stable overexpression of *PFKFB3-4* on the mRNA levels of *PFKFB3-1* and *PFKFB3-11* compared to mock samples. *PFKFB3* mRNA quantity measured as duplicate in three independent experiments (N = 3, n = 2) by quantitative PCR and was normalized to the amount of *TBP* mRNA and compared to mock samples. All values represent the mean ± SEM. All groups were compared using the paired t-test or Mann Whitney test.

https://doi.org/10.1371/journal.pone.0241092.g004

mRNA levels of *PFKFB3-1* and *PFKFB3-11*. Transient overexpression of PFKFB3-5 resulted in an increase of *PFKFB3-1* in both cell lines, whereas an increase in *PFKFB3-11* mRNA was detected exclusively in U87 cells (Fig 5E). The strong increase of *PFKFB3-1* in U87 cells appears to be due to much higher transcriptional level of overexpressed *PFKFB3-5* in these cells compared to HEK-293 cells. Thus, drastic overexpression of PFKFB3-5 impacts the expression level of other PFKFB3 splice variants, indicating their functional interplay.

To test whether the effects of PFKFB3-5 overexpression on cell viability and proliferation are dosage-dependent, we stably overexpressed PFKFB3-5 in HEK-293 and U87 cells. After stable overexpression of PFKFB3-5 we found an increase of mRNA of PFKFB3-5 5 times in HEK-293 cells and 12 times in U87 cells. The protein was increased 4.1 times in HEK-293 cells and 15 times in U87 cells (Fig 6A and 6B, S9 and S10 Appendices). Strikingly, moderate over-expression of PFKFB3-5 has an inhibiting effect on cell viability and proliferation (Fig 6C and 6D). In contrast, high PFKFB3-5 expression level in transiently transfected HEK-293 and U87 cells had no effect on cell viability and proliferation (Fig 5C and 5D). Noticeably, transcript levels of *PFKFB3-1* and *PFKFB3-11* appeared unaltered when PFKFB3-5 are overexpressed under these conditions (Fig 6E). Taken together, our findings prove specific, dose-dependent effects of PFKFB3 splice variants on the growth capacity of tumor cells and HEK-293 cells.

PFKFB3-5 expression is reduced in glioblastomas (IDH-wildtype)

Contradicting previous reports [21], the data presented here support the idea that PFKFB3-4 exerts no growth-inhibiting effect, while PFKFB3-5 inhibits cell proliferation *in vitro*. This begs the question whether the ratio of *PFKFB3-4* to *PFKFB3-5* is relevant for neoplastic traits in glioblastomas. To examine the *PFKFB3-4 to -5* mRNA ratio, we set up a multiplex PCR to simultaneously measure both transcript species in different cell lines including glioblastoma cells and in glioblastoma patient samples. In glioblastoma cell lines (U87, LN405 and 1321N1), the ratio between *PFKFB3-4* to *PFKFB3-5* mRNA was significantly shifted toward *PFKFB3-4* (U87: 80:1; LN405: 5.4:1 and 1321N1: 5.7:1; Fig 7B and 7C, S11 Appendix). Non-glioma cell lines (HEK-293, SH-SYHY) and normal brain tissue samples from the temporal cortex showed a ratio close to 1:1 (HEK-293: 0.65:1; SH-SY5Y: 1.1:1; Fig 7B and 7C, S11 Appendix).

Motivated by these findings, we analyzed the *PFKFB3-4* to *PFKFB3-5* ratio in 30 IDH-wild-type glioblastomas and in 15 normal human brain samples (Fig 7D and 7E, S12 Appendix). We found that *PFKFB3-4* to *PFKFB3-5* ratio in IDH-wildtype glioblastomas (24:1) was about 40-fold higher than in normal brain tissue (1:1.6). Similarly to glioblastoma cell lines, the ratio of *PFKFB3-4* to *PFKFB3-5* in IDH-wildtype glioblastomas was directed towards splice variant *PFKFB3-4*. This is in agreement with our findings that PFKFB3-4 promotes proliferation of U87 cells, whereas PFKFB3-5 has an inhibitory effect on cell proliferation. Hence, low PFKFB3-5 expression levels relative to PFKFB3-4 levels seem to confer growth advantage on glioblastomas.

In sum, our data show that PFKFB3-5 may play a decisive role in growth regulation of glioblastomas.

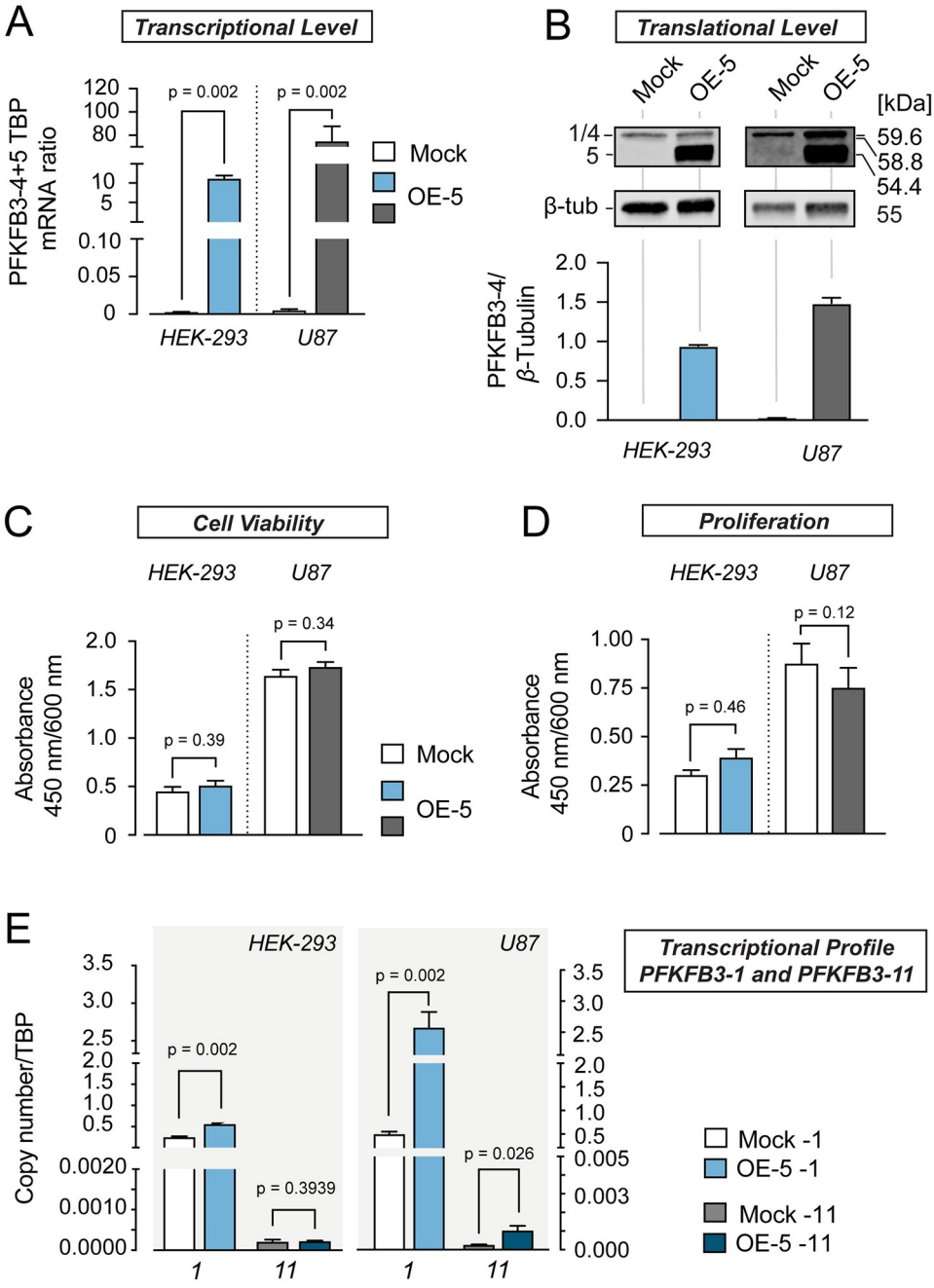

Fig 5. Transient overexpression of PFKFB3-5 has no impact on cell viability and proliferation but changes the transcriptional profile of PFKFB3-1 and -11. (A) Quantification of *PFKFB3-5* mRNA levels from HEK-293 (blue) and U87 cells (grey) transiently overexpressing PFKFB3-5. Cells were harvested 24 h after transfection. *PFKFB3-5* mRNA quantity was compared to mock samples and normalized to the amount of *TBP* mRNA measured by quantitative PCR (N = 3, n = 2). (B) Western blot analysis to confirm the overexpression of PFKFB3-5 with polyclonal PFKFB3 antibody. *β*-Tubulin served as loading control, 10 μg protein were loaded per lane. Cells were harvested 48 h after transfection. The ratio of protein bands (PFKFB3-5 to *β*-Tubulin) was calculated from the intensity values of protein bands (n = 3). (C) Effect of PFKFB3-5 overexpression on cell viability, measured by WST-1 assay. Cells were harvested 24 hours after transfection. After a 4 h incubation period with WST-1 reagent the absorbance was measured at 450 nm/600 nm (N = 7, n = 7–8). (D) Effect of PFKFB3-5 overexpression on proliferation measured by BrdU-assay. Cells were harvested 24 h after transfection. After an 20 h incubation period with BrdU, the absorbance was measured at 450 nm/600 nm (N = 7, n = 7). (E) Impact of transient overexpression of *PFKFB3-5* on the mRNA levels of *PFKFB3-1* and *PFKFB3-11*. Cells were harvested 24 h after transfection. The quantity of *PFKFB3* mRNA was measured as duplicate (n = 2) in three independent experiments (N = 3) by quantitative PCR and was normalized to the amount of *TBP* mRNA. Values represent the mean ± SEM. Groups were compared using the paired t-test or Mann Whitney test.

https://doi.org/10.1371/journal.pone.0241092.g005

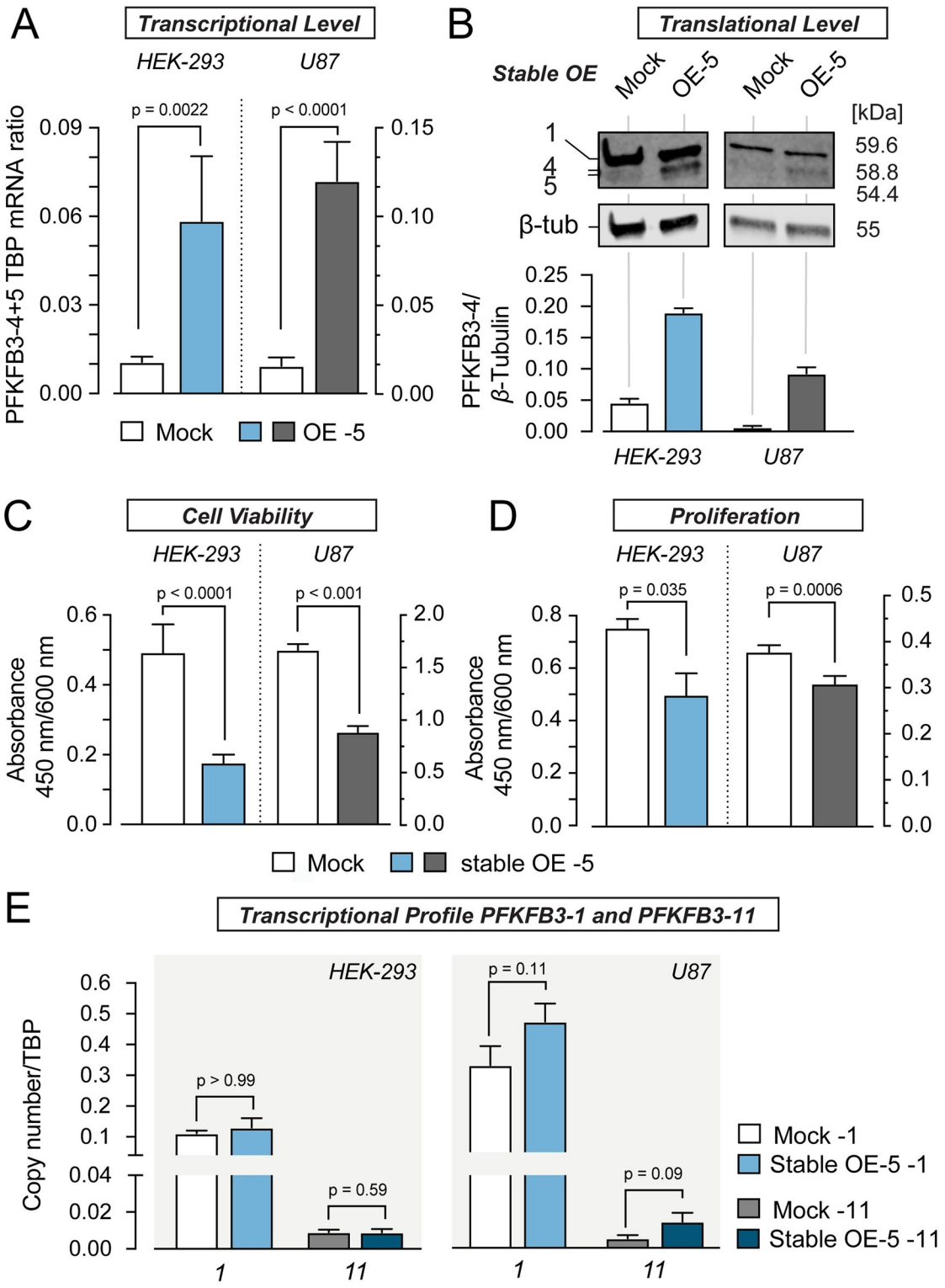

Fig 6. Stable overexpression of PFKFB3-5 in HEK-293 and U87 cells leads to decreased cell viability and proliferation while leaving transcriptional profile of PFKFB3-1 and -11 unaltered. (A) Quantification of *PFKFB3-5* mRNA levels from HEK-293 (blue) and U87 (grey) cells stably overexpressing *PFKFB3-5* (OE -5). *PFKFB3-5* mRNA quantity was normalized to the amount of *TBP* mRNA measured by quantitative PCR and compared to mock samples (for HEK-293: N = 3, n = 2, for U87: N = 4, n = 3). (B) Shows western blot analysis to confirm the overexpression of PFKFB3-5 with polyclonal PFKFB3 antibody. *β*-Tubulin served as loading control, 10 μg protein were loaded per lane. 1 means PFKFB3-1 and 4 PFKFB-4. The ratio of protein bands (PFKFB3-5 to *β*-

Tubulin) was calculated from the intensity values of protein bands (n = 3). (C) Effect of stable PFKFB3-5 overexpression on cell viability, measured by WST-1 assay. After a 4 h incubation period with WST-1 reagent the absorbance was measured at 450 nm/ 600 nm (N = 4, n = 5–7). (D) Effect of stable PFKFB3-5 overexpression on proliferation measured by BrdU-assay. After 20 h incubation period with BrdU, the absorbance was measured at 450 nm/600 nm (N = 3, n = 6–8). (E) Influence of stable overexpression of PFKFB3-5 on the mRNA levels of PFKFB3-1 and PFKFB3-11 compared to mock samples (N = 3, n = 2 for HEK-293 cells and N = 4, n = 3 for U87 cells). All values represent the mean ± SEM. All groups were compared using the paired t-test or Mann Whitney test.

https://doi.org/10.1371/journal.pone.0241092.g006

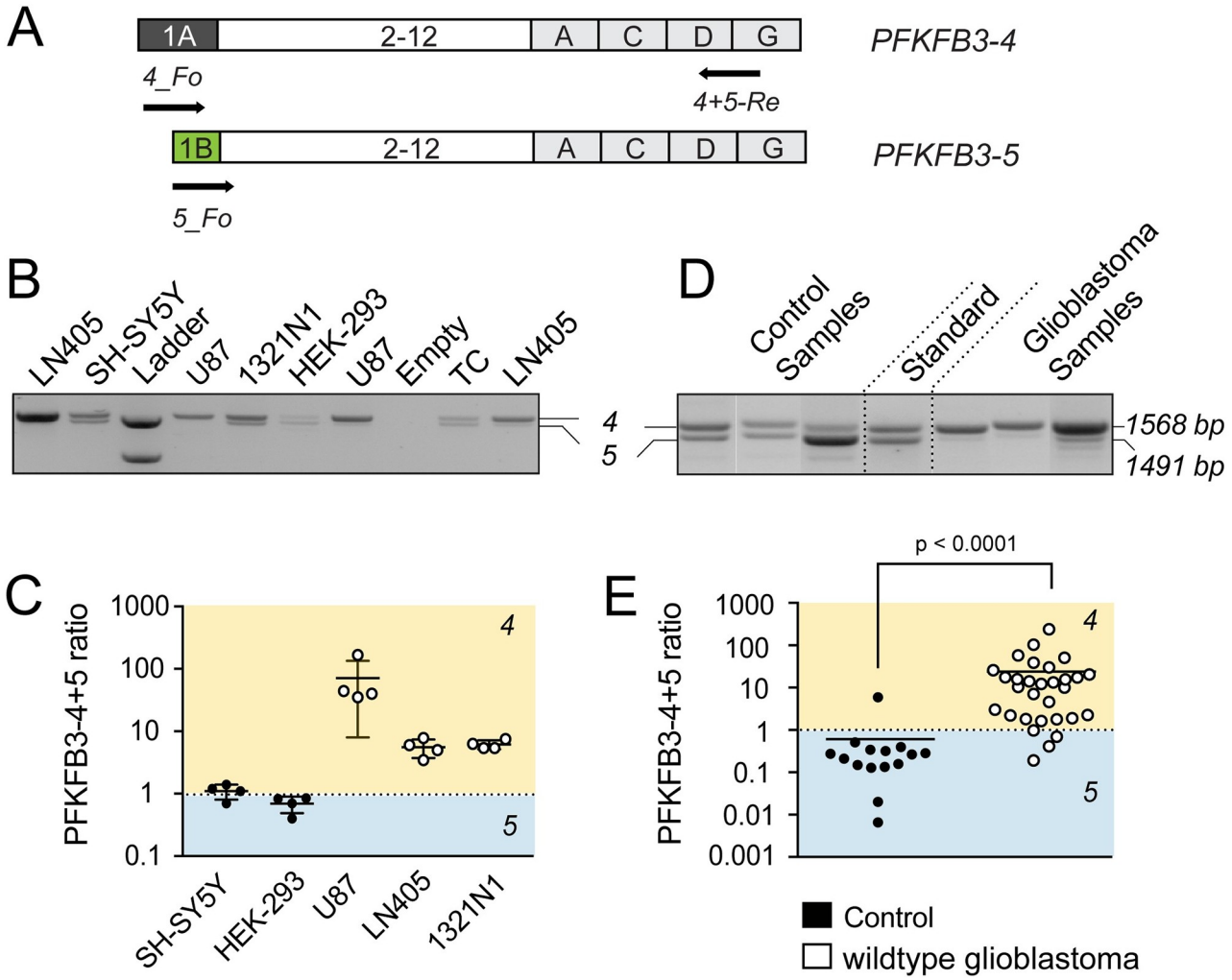

Fig 7. Glioblastoma cell lines and wildtype glioblastomas are signified by high PFKFB3-4 to PFKFB3-5 ratio. (A) Schematic illustration of experimental design of multiplex PCR used to measure the *PFKFB3-4* to *PFKFB3-5* mRNA ratio in different cell lines (B,C) and brain samples from patients (D,E). (B) Multiplex PCR products from several cell lines and human temporal cortex (TC) were separated by agarose gel electrophoresis. Equal amounts of mRNA of *PFKFB3-4* and *PFKFB3-5* (10^7 copies) were used as a standard (1568 bp and 1491 bp). (C) Scatter dot blot of *PFKFB3-4* to *PFKFB-5* mRNA ratios calculated from fluorescence intensities of *PFKFB3-4* (1568 bp) and *PFKFB3-5* (1491 bp) fragments (n = 4). (D) Agarose gel electrophorese of multiplex PCR products from three representative normal tissue as control samples and three IDH-wildtype glioblastomas. Equal amounts of mRNA from *PFKFB3-4 and PFKFB3-5* (10^7 copies) were used as a standard. (E) Fluorescence intensities of multiplexed PCR fragments from 15 control and 30 samples from IDH-wildtype glioblastoma patients were used to quantify the ratio of *PFKFB3-4* to *PFKFB3-5*. Similar to cell lines, fast-proliferating glioblastoma samples from patients tend to show higher PFKFB3-4 expression. All groups were compared using the Mann Whitney test.

https://doi.org/10.1371/journal.pone.0241092.g007

Discussion

High rates of glycolysis constitute a prerequisite to sustaining the metabolic demands of glioblastomas. The PFKFB3 isozymes have been identified as one of the major metabolic players in glioblastoma however, thus far the functional relevance of PFKFB3 splice variants is only partially understood. The consequences of the different C- and N- terminal structures of PFKFB3 splice variants on their individual functions are unknown. However, the tissue-dependent expression pattern of these splice variants [16] point to their specific functional/regulatory roles in cell metabolism. In humans, at least eleven different *PFKFB3* transcripts (*PFKFB3-1-11*) are known. In glioblastomas only three *PFKFB3* transcripts -1, -4 and -11 (former UBI2K4, 5 and 6) were detected, with decreased mRNA levels documented for *PFKFB3-4* [20, 21], compared to low-grade astrocytomas and normal brain tissue. Moreover, overexpression of PFKFB3-4 fusion protein blunted cell viability and anchorage-independent growth of U87 cells, and its expression level inversely correlated with the growth rate of several human cancer cell lines [21]. Consistent with the idea that PFKFB3-4 possesses tumor inhibiting features, the loss-of-heterozygosity (LOH) of the *PFKFB3* gene locus, which negatively affects the prognosis of glioblastoma patients was identified [7]. Following this rationale, we expected that knockdown of *PFKFB3-4* with si/shRNA should elevate cell growth. Contrarily, we found that knockdown of *PFKFB3-4+5* in U87 and HEK-293 cells results in decreased cell viability and cell proliferation when compared to control samples. Note that the shRNA and siRNA probes used in this study were directed against the C-terminal stretch, the sequence of which is indistinguishable between PFKFB3-4 and PFKFB3-5 (Fig 2A), thus both variants were affected simultaneously. Stably and transiently transfected HEK-293 cells were used for quantification of cell viability (Fig 2D), whereas U87 cells were transfected only with siRNA. The knockdown in HEK-293 cells was stronger compared to U87 cells. This could explain differences in cell viability after knockdown of *PFKFB3-4+5*. Additionally, the mRNA level in HEK-293 cells was higher than in U87 cells. For quantification of cell growth by cell counting (Fig 3A) only stably transfected HEK-293 cells were used. The knockdown in stably and transiently transfected HEK-293 cells was stronger than in cells only stably transfected (data not shown) resulting the difference between Figs 2D and 3A. The discrepancy between the growth inhibiting effects induced by *PFKFB3-4+5* knockdown, as well as the overexpression of the PFKFB3-4 fusion protein requires a more detailed investigation of PFKFB3-4 in the glioblastoma context, especially with regard to the putative effects of biochemical tag fusion [29].

To mimic (patho)physiological conditions more closely, native PFKFB3-4 was stably overexpressed in HEK-293 and U87 cells. We found increased viability and proliferation of both cell lines compared to control cells with empty vector, indicating growth promoting effects of PFKFB3-4 (Fig 4C and 4D). This is in line with the blunted growth in PFKFB3-4+5-deficient HEK-293 and U87 cells (Fig 2D and 2E), strongly arguing against the tumor-suppressive role and rather suggesting tumor-promoting effects of PFKFB3-4. Paradoxically, PFKFB3-4 expression was shown to be reduced in glioblastoma samples versus low-grade astrocytomas and normal brain tissue [21]. This may be reconciled by the fact that the qPCR oligonucleotides target not only *PFKFB3-4* mRNA, but also *PFKFB3-5* mRNA (Fig 2A), the sequence of which was only recently published in the NCBI database (NM 001323016.2). Therefore, we turned our attention to the investigation of PFKFB3-5 function in glioblastoma. Transient overexpression of PFKFB3-5 in both HEK-293 and U87 cells left viability and proliferation unaltered (Fig 5C and 5D), but led to a significant increase in *PFKFB3-1*, an effect not detectable when PFKFB3-4 was stably overexpressed (Fig 4E). PFKFB3-1 constitutes the best studied and most abundant PFKFB splice variant in tumor cells known to promote tumorigenic progression [30]. Fig 5A indicates that the transcriptional level of PFKFB-5 when overexpressed in HEK

cells is lower compared to U87 cells. In addition, on protein level the effect in U87 cells are higher. Increase in *PFKFB3-1* observed in PFKFB3-5 overexpressing cells probably compensates for the growth-inhibiting effect of PFKFB3-5 and, thus, viability and proliferation of these cells do not change in sum compared to mock cells (Fig 5C and 5D). The strong increase of *PFKFB3-1* in U87 cells seems to be due to the much higher transcriptional level of *PFKFB3-5* in these cells compared to HEK-293 cells. This is in line with the notion that PFKFB-1 to some extent acts to balance the effects mediated by PFKFB3-5. The increase of the *PFKFB3-11* transcriptional level in PFKFB3-5 overexpressing U87 cells cannot be explained yet. PFKFB3-11 has no nuclear localization signal and should only have glycolytic functions. The increase of mRNA could be a part of the adaptive mechanism of cells to maintain their growth rate.

Similar to stable overexpression of PFKFB3-4 we generated a HEK-293 and U87 cell line stably overexpressing PFKFB3-5. Compared to the transient overexpression the effect on mRNA and protein level was much less pronounced. Strikingly, cell viability and proliferation were decreased in these cells compared to control cells (Fig 6C and 6D), while *PFKFB3-1* and *-11* levels remained unaltered (Fig 6E). The effect of stable overexpression of PFKFB3-5 on proliferation in U87 cells is less reduced compared to HEK-293 cells. This can be related to the small but not significant increase of *PFKFB3-1* and *PFKFB3-11* in these cells. In conclusion, our data suggest that PFKFB3-5 mediates growth inhibiting effects *in vitro*, while PFKFB3-4 exerts the opposite effect on tumor cell growth. In summary, these results underscore that data derived from exogenous cell systems should be carefully interpreted and the findings should be validated ideally in more native experimental settings. To this end, we quantified the *PFKFB3-4* to *PFKFB3-5* ratio in different cell lines varying in their proliferation features. Interestingly, astrocytoma cell lines like U87, LN-405 or 1321N1 lines contain more *PFKFB3-4* than *PFKFB3-5* mRNA, while the *PFKFB3-4* to *-5* ratio is close to 1:1 in non-glioma cell lines (Fig 7B and 7C). Next, we collected glioblastoma and normal brain samples from patients and scored the *PFKFB3-4* to *-5* ratio. In IDH-wildtype glioblastomas we also found a significant shift towards *PFKFB3-4* expression compared to *PFKFB3-5* (Fig 7D and 7E), whereas the *PFKFB3-4* to *-5* ratio in normal brain tissue was also near 1:1. In conclusion, increased proliferation rates in highly malignant glioblastomas as well as in glioblastoma cell lines might be causally related to the high *PFKFB3-4* to *-5* expression ratio in which PFKFB3-4 is showing strong growth promoting effects. Our data indicate that, in addition to the well-established pro-proliferating role of PFKFB3-1 [31], also PFKFB3-4 acts as a growth-promoting factor in in glioblastomas.

In order to understand the function of PFKFB3 splice variants their molecular structure has to be contemplated. The enzymatic core of PFKFB3 can be regulated by a variety of different mechanisms [32]. The only structural distinction between PFKFB3-4 and -5 can be found within the N-terminus, which is typically not post-translationally modified. PFKFB3-5 has a comparably short N-terminus containing only five amino acids, whereas PFKFB3-4 contains 26 amino acids (Fig 1). Based on the crystal structure of PFKFB3 [33] it has been hypothesized that the N-terminus exerts an autoinhibitory effect on PFKFB3 bisphosphatase activity. Bisphosphatase inhibition may thus be relieved to some extent in PFKFB3-5. In accordance with this model a 7-fold higher phosphatase activity was observed for N-terminally truncated versions PFKFB3 [34]. Inversely, it would be interesting to investigate the enzymatic profile of PFKFB3-3, which contains the longest N-terminus amongst PFKFB3 splice variants.

The question remains why glioblastoma cells tend to express less PFKFB3-5. Further, it would be intriguing to study if gliomablastoma cells tend to switch to the expression of splice variants with longer N-termini to ensure an elevation in kinase activity.

Detailed knowledge of putative biochemical differences of PFKFB3 splice variants is scarce. Here, we show that two PFKFB3 splice variants exert different effects on growth rates of cell culture, possibly associated to the structural variation of their N-termini.

Several small molecule inhibitors of PFKFB3 have been developed, although their application to cancer treatment has been limited since tumor cells have developed unique survival strategies to antagonize inhibition of glucose metabolism [35]. More recently, alternative approaches aiming at pharmacological control of PFKFB3's phosphatase activity were developed and await testing in clinical settings [36, 37]. A ß-hairpin interaction of PFKFB3's N-terminus and the phosphatase domain seem to be a structural prerequisite for the autoinhibitory function PFKFB3. Building on this characteristic it was shown that pharmaceutical disruption of this structural element may serve as a handle to increase phosphatase activity [37], which may have the capacity to pave the way towards novel pharmaceutical avenues to treat cancer.

However, the PFKFB3 is embedded in a complex highly regulated metabolic system. In this regard, it should also be mentioned that other PFKFB isoenzymes, especially PFKFB4, shape the adaptation of tumor cell metabolism [38].

In conclusion, we provide experimental and clinical evidence suggesting the significance of a specific PFKFB3 splice variant (PFKFB3-4) as a growth promoting factor in glioblastoma. In addition, here we first report on the role of the novel splice variant PFKFB3-5 in glioblastoma, which contrasts the prevailing growth-promoting function of PFKFB3. Furthermore, our data suggest that the adaptation and survival of tumor cells is shaped by the expression changes of these specific splice variants, a feature that may constitute a first step towards the development of a novel prognostic parameter in glioblastoma.

Supporting information

S1 Appendix. Knock-down of PFKFB3-4+5 alters proliferation and viability of HEK-293 cells. Western blot analysis of PFKFB3 protein expression following si/shRNA mediated PFKFB3-4+5 knock-down utilizing polyclonal PFKFB3 antibody. Proteins were detected 48 h after siRNA treatment. β-Tubulin served as loading control. **Raw image**: S1 Appendix.
(TIF)

S2 Appendix. Knock-down of PFKFB3-4+5 alters proliferation and viability of U87 cells. Western blot analysis of PFKFB3 protein expression following si/shRNA mediated PFKFB3-4+5 knock-down utilizing polyclonal PFKFB3 antibody. Proteins were detected 48 h after siRNA treatment. β-Tubulin served as loading control. **Raw image**: S2 Appendix.
(TIF)

S3 Appendix. PFKFB3-4+5 knockdown leads to decreased cell growth and colony formation. Representative brightfield image of scr-shRNA and 4+5 shRNA treated HEK-293 cells cultured in 12-well plates. Image was taken after 5 d of cell seeding. **Raw image:** S3 Appendix.
(TIF)

S4 Appendix. PFKFB3-4+5 knockdown leads to decreased cell growth and colony formation. Representative images of soft agar colonies formed by HEK-293 cells (scr-shRNA) and HEK-293 cells with stably reduced PFKFB3-4+5 levels (4/5 shRNA). The cells (5000 cells) were cultured for 14 d in 6-well plates on soft agar. **Raw image:** S4 Appendix.
(TIF)

S5 Appendix. PFKFB3-4 overexpression facilitates cell viability and proliferation of HEK-293 cells. Western blot analysis to confirm overexpression of PFKFB3-4 with polyclonal PFKFB3 antibody. β-Tubulin served as loading control. **Raw image:** S5 Appendix.
(TIF)

S6 Appendix. PFKFB3-4 overexpression facilitates cell viability and proliferation of U87 cells. Western blot analysis to confirm the overexpression of PFKFB3-4 with polyclonal

PFKFB3 antibody. β-Tubulin served as loading control. **Raw image:** S6 Appendix.
(TIF)

S7 Appendix. Transient overexpression of PFKFB3-5 in HEK-293 cells has no impact on cell viability and proliferation, but changes the transcriptional profile of PFKFB3-1 and -11. Western blot analysis to confirm the overexpression of PFKFB3-5 with polyclonal PFKFB3 antibody. β-Tubulin served as loading control. **Raw image:** (S7 Appendix).
(TIF)

S8 Appendix. Transient overexpression of PFKFB3-5 in U87 cells has no impact on cell viability and proliferation but changes the transcriptional profile of PFKFB3-1 and -11. Western blot analysis to confirm the overexpression of PFKFB3-5 with polyclonal PFKFB3 antibody. β-Tubulin served as loading control. **Raw image:** S8 Appendix.
(TIF)

S9 Appendix. Stable overexpression of PFKFB3-5 in HEK-293 cells leads to decreased cell viability and proliferation while leaving transcriptional profile of PFKFB3-1 and -11 unaltered. Western blot analysis to confirm the overexpression of PFKFB3-5 with polyclonal PFKFB3 antibody. β-Tubulin served as loading control. **Raw image:** S9 Appendix.
(TIF)

S10 Appendix. Stable overexpression of PFKFB3-5 in U87 cells leads to decreased cell viability and proliferation while leaving transcriptional profile of PFKFB3-1 and -11 unaltered. Western blot analysis to confirm the overexpression of PFKFB3-5 with polyclonal PFKFB3 antibody. β-Tubulin served as loading control. **Raw image:** S10 Appendix.
(TIF)

S11 Appendix. Glioblastoma cell lines contain a high PFKFB3-4 to PFKFB3-5 ratio. Multiplex PCR products from several cell lines and human temporal cortex (TC) were separated by agarose gel electrophoresis. Equal amounts of mRNA of *PFKFB3-4* and *PFKFB3-5* (10^7 copies) were used as a standard (1568 bp and 1491 bp). Basis for data shown in Fig 7B and 7C. **Raw image:** S11 Appendix.
(TIF)

S12 Appendix. Glioblastoma samples from patients contain a high PFKFB3-4 to PFKFB3-5 ratio. Agarose gel electrophorese of multiplex PCR products healthy tissue as control samples and IDH-wildtype glioblastomas. Equal amounts of mRNA from *PFKFB3-4 and PFKFB3-5* (10^7 copies) were used as a standard. Basis for data shown in Fig 7D and 7E. **Raw images:** S12 Appendix.
(TIF)

S1 Table. Summarizes tumor and control samples.
(PDF)

S2 Table. Lists primers and oligonucleotides used.
(PDF)

S3 Table. This table shows siRNAs used.
(PDF)

Acknowledgments

We thank Andrea Boehme for technical assistance as well as Helen Middleton-Price and Tobias Langenhan for discussions.

Author Contributions

Conceptualization: Renate Kessler, Marina Bigl.

Data curation: Marina Bigl.

Formal analysis: Ulli Heydasch, Renate Kessler, Jan-Peter Warnke, Marina Bigl.

Funding acquisition: Renate Kessler, Nicole Scholz.

Investigation: Renate Kessler, Marina Bigl.

Methodology: Ulli Heydasch, Renate Kessler, Marina Bigl.

Project administration: Marina Bigl.

Resources: Jan-Peter Warnke.

Supervision: Marina Bigl.

Validation: Marina Bigl.

Writing – original draft: Nicole Scholz, Marina Bigl.

Writing – review & editing: Renate Kessler, Klaus Eschrich, Nicole Scholz, Marina Bigl.

References

1. Agnihotri S, Zadeh G. Metabolic reprogramming in glioblastoma: the influence of cancer metabolism on epigenetics and unanswered questions. Neuro Oncol. 2016; 18(2):160–72. https://doi.org/10.1093/neuonc/nov125 PMID: 26180081
2. Bartrons R, Simon-Molas H, Rodríguez-García A, Castaño E, Navarro-Sabaté À, Manzano A, et al. Fructose 2,6-Bisphosphate in Cancer Cell Metabolism. Front Oncol. 2018; 8:331. Epub 2018/09/21. https://doi.org/10.3389/fonc.2018.00331 PMID: 30234009
3. Van Schaftingen E, Jett MF, Hue L, Hers HG. Control of liver 6-phosphofructokinase by fructose 2,6-bisphosphate and other effectors. Proc Natl Acad Sci U S A. 1981; 78(6):3483–6. https://doi.org/10.1073/pnas.78.6.3483 PMID: 6455662
4. Pilkis SJ, Claus TH, Kurland IJ, Lange AJ. 6-Phosphofructo-2-kinase/fructose-2,6-bisphosphatase: a metabolic signaling enzyme. Annu Rev Biochem. 1995; 64:799–835. https://doi.org/10.1146/annurev.bi.64.070195.004055 PMID: 7574501
5. Okar DA, Manzano A, Navarro-Sabate A, Riera L, Bartrons R, Lange AJ. PFK-2/FBPase-2: maker and breaker of the essential biofactor fructose-2,6-bisphosphate. Trends Biochem Sci. 2001; 26(1):30–5. https://doi.org/10.1016/s0968-0004(00)01699-6 PMID: 11165514
6. Sakakibara R, Kato M, Okamura N, Nakagawa T, Komada Y, Tominaga N, et al. Characterization of a human placental fructose-6-phosphate, 2-kinase/fructose-2,6-bisphosphatase. J Biochem. 1997; 122 (1):122–8. https://doi.org/10.1093/oxfordjournals.jbchem.a021719 PMID: 9276680
7. Fleischer M, Kessler R, Klammer A, Warnke JP, Eschrich K. LOH on 10p14-p15 targets the PFKFB3 gene locus in human glioblastomas. Genes Chromosomes Cancer. 2011; 50(12):1010–20. https://doi.org/10.1002/gcc.20914 PMID: 21987444
8. Chesney J. 6-phosphofructo-2-kinase/fructose-2,6-bisphosphatase and tumor cell glycolysis. Curr Opin Clin Nutr Metab Care. 2006; 9(5):535–9. https://doi.org/10.1097/01.mco.0000241661.15514.fb PMID: 16912547
9. Bolanos JP. Adapting glycolysis to cancer cell proliferation: the MAPK pathway focuses on PFKFB3. Biochem J. 2013; 452(3). https://doi.org/10.1042/BJ20130560 PMID: 23725459
10. Obach M, Navarro-Sabate A, Caro J, Kong X, Duran J, Gomez M, et al. 6-Phosphofructo-2-kinase (pfkfb3) gene promoter contains hypoxia-inducible factor-1 binding sites necessary for transactivation in response to hypoxia. J Biol Chem. 2004; 279(51):53562–70. https://doi.org/10.1074/jbc.M406096200 PMID: 15466858
11. Yalcin A, Clem BF, Simmons A, Lane A, Nelson K, Clem AL, et al. Nuclear targeting of 6-phosphofructo-2-kinase (PFKFB3) increases proliferation via cyclin-dependent kinases. J Biol Chem. 2009; 284 (36):24223–32. https://doi.org/10.1074/jbc.M109.016816 PMID: 19473963

12. Yalcin A, Clem BF, Imbert-Fernandez Y, Ozcan SC, Peker S, O'Neal J, et al. 6-Phosphofructo-2-kinase (PFKFB3) promotes cell cycle progression and suppresses apoptosis via Cdk1-mediated phosphorylation of p27. Cell Death Dis. 2014; 17(5):292. https://doi.org/10.1038/cddis.2014.292 PMID: 25032860

13. Kaplon J, van Dam L, Peeper D. Two-way communication between the metabolic and cell cycle machineries: the molecular basis. Cell Cycle. 2015; 14(13):2022–32. https://doi.org/10.1080/15384101.2015.1044172 PMID: 26038996

14. Jia W, Zhao X, Zhao L, Yan H, Li J, Yang H, et al. Non-canonical roles of PFKFB3 in regulation of cell cycle through binding to CDK4. Oncogene. 2018; 37(13):1685–98. https://doi.org/10.1038/s41388-017-0072-4 PMID: 29335521

15. Gustafsson NMS, Farnegardh K, Bonagas N, Ninou AH, Groth P, Wiita E, et al. Targeting PFKFB3 radiosensitizes cancer cells and suppresses homologous recombination. Nat Commun. 2018; 9(1):018–06287. https://doi.org/10.1038/s41467-018-06287-x PMID: 30250201

16. Roy D, Sheng GY, Herve S, Carvalho E, Mahanty A, Yuan S, et al. Interplay between cancer cell cycle and metabolism: Challenges, targets and therapeutic opportunities. Biomed Pharmacother. 2017; 89:288–96. https://doi.org/10.1016/j.biopha.2017.01.019 PMID: 28235690

17. Kessler R, Eschrich K. Splice isoforms of ubiquitous 6-phosphofructo-2-kinase/fructose-2,6-bisphosphatase in human brain. Brain Res Mol Brain Res. 2001; 87(2):190–5. https://doi.org/10.1016/s0169-328x(01)00014-6 PMID: 11245921

18. Bando H, Atsumi T, Nishio T, Niwa H, Mishima S, Shimizu C, et al. Phosphorylation of the 6-phosphofructo-2-kinase/fructose 2,6-bisphosphatase/PFKFB3 family of glycolytic regulators in human cancer. Clin Cancer Res. 2005; 11(16):5784–92. https://doi.org/10.1158/1078-0432.CCR-05-0149 PMID: 16115917

19. Calvo MN, Bartrons R, Castano E, Perales JC, Navarro-Sabate A, Manzano A. PFKFB3 gene silencing decreases glycolysis, induces cell-cycle delay and inhibits anchorage-independent growth in HeLa cells. FEBS Lett. 2006; 580(13):3308–14. https://doi.org/10.1016/j.febslet.2006.04.093 PMID: 16698023

20. Kessler R, Bleichert F, Warnke JP, Eschrich K. 6-Phosphofructo-2-kinase/fructose-2,6-bisphosphatase (PFKFB3) is up-regulated in high-grade astrocytomas. J Neurooncol. 2008; 86(3):257–64. https://doi.org/10.1007/s11060-007-9471-7 PMID: 17805487

21. Zscharnack K, Kessler R, Bleichert F, Warnke JP, Eschrich K. The PFKFB3 splice variant UBI2K4 is downregulated in high-grade astrocytomas and impedes the growth of U87 glioblastoma cells. Neuropathology and Applied Neurobiology. 2009; 35(6):566–78. https://doi.org/10.1111/j.1365-2990.2009.01027.x PMID: 19490427

22. Manzano A, Rosa JL, Ventura F, Perez JX, Nadal M, Estivill X, et al. Molecular cloning, expression, and chromosomal localization of a ubiquitously expressed human 6-phosphofructo-2-kinase/ fructose-2, 6-bisphosphatase gene (PFKFB3). Cytogenet Cell Genet. 1998; 83(3–4):214–7. https://doi.org/10.1159/000015181 PMID: 10072580

23. Sakai A, Kato M, Fukasawa M, Ishiguro M, Furuya E, Sakakibara R. Cloning of cDNA encoding for a novel isozyme of fructose 6-phosphate, 2-kinase/fructose 2,6-bisphosphatase from human placenta. J Biochem. 1996; 119(3):506–11. https://doi.org/10.1093/oxfordjournals.jbchem.a021270 PMID: 8830046

24. Hamilton JA, Callaghan MJ, Sutherland RL, Watts CK. Identification of PRG1, a novel progestin-responsive gene with sequence homology to 6-phosphofructo-2-kinase/fructose-2,6-bisphosphatase. Mol Endocrinol. 1997; 11(4):490–502. https://doi.org/10.1210/mend.11.4.9909 PMID: 9092801

25. Chesney J, Mitchell R, Benigni F, Bacher M, Spiegel L, Al-Abed Y, et al. An inducible gene product for 6-phosphofructo-2-kinase with an AU-rich instability element: role in tumor cell glycolysis and the Warburg effect. Proc Natl Acad Sci U S A. 1999; 96(6):3047–52. https://doi.org/10.1073/pnas.96.6.3047 PMID: 10077634

26. Louis DN, Perry A, Reifenberger G, von Deimling A, Figarella-Branger D, Cavenee WK, et al. The 2016 World Health Organization Classification of Tumors of the Central Nervous System: a summary. Acta Neuropathol. 2016; 131(6):803–20. https://doi.org/10.1007/s00401-016-1545-1 PMID: 27157931

27. Hartmann C, Meyer J, Balss J, Capper D, Mueller W, Christians A, et al. Type and frequency of IDH1 and IDH2 mutations are related to astrocytic and oligodendroglial differentiation and age: a study of 1,010 diffuse gliomas. Acta Neuropathol. 2009; 118(4):469–74. https://doi.org/10.1007/s00401-009-0561-9 PMID: 19554337

28. van de Wetering M, Oving I, Muncan V, Pon Fong MT, Brantjes H, van Leenen D, et al. Specific inhibition of gene expression using a stably integrated, inducible small-interfering-RNA vector. EMBO Rep. 2003; 4(6):609–15. https://doi.org/10.1038/sj.embor.embor865 PMID: 12776180

29. Mohanty AK, Wiener MC. Membrane protein expression and production: effects of polyhistidine tag length and position. Protein Expr Purif. 2004; 33(2):311–25. https://doi.org/10.1016/j.pep.2003.10.010 PMID: 14711520

30. Atsumi T, Chesney J, Metz C, Leng L, Donnelly S, Makita Z, et al. High expression of inducible 6-phosphofructo-2-kinase/fructose-2,6-bisphosphatase (iPFK-2; PFKFB3) in human cancers. Cancer Res. 2002; 62(20):5881–7. PMID: 12384552

31. Shi L, Pan H, Liu Z, Xie J, Han W. Roles of PFKFB3 in cancer. Signal Transduct Target Ther. 2017; 2 (17044). https://doi.org/10.1038/sigtrans.2017.44 PMID: 29263928

32. Yi M, Ban Y, Tan Y, Xiong W, Li G, Xiang B. 6-Phosphofructo-2-kinase/fructose-2,6-biphosphatase 3 and 4: A pair of valves for fine-tuning of glucose metabolism in human cancer. Mol Metab. 2019; 20:1–13. https://doi.org/10.1016/j.molmet.2018.11.013 PMID: 30553771

33. Kim SG, Manes NP, El-Maghrabi MR, Lee YH. Crystal structure of the hypoxia-inducible form of 6-phosphofructo-2-kinase/fructose-2,6-bisphosphatase (PFKFB3): a possible new target for cancer therapy. J Biol Chem. 2006; 281(5):2939–44. https://doi.org/10.1074/jbc.M511019200 PMID: 16316985

34. Manes NP, El-Maghrabi MR. The kinase activity of human brain 6-phosphofructo-2-kinase/fructose-2,6-bisphosphatase is regulated via inhibition by phosphoenolpyruvate. Arch Biochem Biophys. 2005; 438(2):125–36. https://doi.org/10.1016/j.abb.2005.04.011 PMID: 15896703

35. Bartrons R, Rodriguez-Garcia A, Simon-Molas H, Castano E, Manzano A, Navarro-Sabate A. The potential utility of PFKFB3 as a therapeutic target. Expert Opin Ther Targets. 2018; 16:1–16. https://doi.org/10.1080/14728222.2018.1498082 PMID: 29985086

36. Hanahan D, Weinberg RA. Hallmarks of cancer: the next generation. Cell. 2011; 144(5):646–74. https://doi.org/10.1016/j.cell.2011.02.013 PMID: 21376230

37. Macut H, Hu X, Tarantino D, Gilardoni E, Clerici F, Regazzoni L, et al. Tuning PFKFB3 Bisphosphatase Activity Through Allosteric Interference. Sci Rep. 2019; 9(1):019–56708. https://doi.org/10.1038/s41598-019-56708-0 PMID: 31889092

38. Rider MH, Bertrand L, Vertommen D, Michels PA, Rousseau GG, Hue L. 6-phosphofructo-2-kinase/fructose-2,6-bisphosphatase: head-to-head with a bifunctional enzyme that controls glycolysis. Biochem J. 2004; 381(Pt 3):561–79. https://doi.org/10.1042/BJ20040752 PMID: 15170386